Published by :
http://www.ijert.org

International Journal of Engineering Research & Technology (IJERT)
ISSN: 2278-0181
Vol. 13 Issue 08, August-2024

Impact of Cavity Design on the Efficacy of Charge Plasma TFET-Based Biosensors

Thoti Manoj Kumar
Department of Electronics and Communication Engineering
Koneru Lakshmaiah Education Foundation
Green Fields, Vaddeswaram, 522302

Batchu Lohith
Department of Electronics and Communication Engineering
Koneru Lakshmaiah Education Foundation
Green Fields, Vaddeswaram, 522302

Ammineni Ajay
Department of Electronics and Communication Engineering
Koneru Lakshmaiah Education Foundation
Green Fields, Vaddeswaram, 522302

G.R.K. Prasad
Associate Professor, Department of ECE
Koneru Lakshmaiah Education Foundation
Green Fields, Vaddeswaram, 522302

***Abstract*—In this paper, the application of Tunnelling Field Effect Transistors (TFETs) has been discussed below. The two biosensors that we have proposed are the Cavity on Source Charge Plasma TFET biosensor and the Cavity on Drain Charge Plasma TFET. We measured the drain current for both the biosensors as described above. There is not much difference between the two proposed devices (CS-CPTFET and CD-CPTFET) different being the slight differences in the performance of the devices in terms of drain current. In this study, the performance and validation of the proposed devices are investigated by the Silvaco TCAD simulation tool.**

***Keywords*— TFET Biosensor, charge plasma source, drain, sensitivity, bio molecules**

I. INTRODUCTION

It is a hard task in the medical fraternity to identify diseases at the early stage and indeed ascertain them. The conventional label-based strategies for detecting biomolecules such as electrochemical labeling, fluorescent labeling, and magnetic labeling have some problems as follows: they modify the properties of a biomolecule, which brings about incorrect records and considerable time for reactions [1]. Therefore, researchers have shifted plenty of focus on to the label-free electrical based detection that is accurate and has emerged as the subject of research [2]. FET biosensors have recently been identified as the most effective label-free electrical biomolecule detection solution [3]. These devices have many applications, some of them include food processing, monitoring the environment, and medical diagnosis. When developing biosensors, it is important to consider parameters such as identification speed and sensitivity. There are several advantages of FET-based biosensors such as that the device is very small in size, relatively cheap, and many of them can be manufactured at the same time [4]. The first biosensor based on the FET was named ion-sensitive field-effect transistor (ISFET), which was developed by Bergveld in 1970 [5]. ISFETs are extremely sensitive in charged biomolecules' detection as a problem arises as to whether a biomolecule must come between the electrolyte and electrode, in case of neutral biomolecules. To mitigate this, dielectrically modulated FETs (DMFETs) [6] have been synthesized including the silicon nanowire FET, the FinFET [7], the MOSFET [8-9], and the impact ionization FET [10]. DMFETs [19-23] function based on how the electric characteristics of a device or material alter when biomolecules display dissimilar attributes such as dielectric constant (k) and charge density (Nf) [24-25]. The good interface between the gate and channel enhances the performance of DMFETs.

The problem comes into existence due to primary issues like poor performance, high power consumption and reduced functionality when the MOSFETs are scaled down with the help of technology and miniaturization of the devices become basic for material efficiency. To overcome these challenges, Tunneling Field-Effect Transistors (TFETs) have been effective substitutes in specific fields such as biosensors, which minimizes energy consumption, increases the speed of response and sensitivity. In this research work, a new biosensor is proposed based on a source charge plasma [26-29] TFET with the CPP doping-less approach in which device manufacturing relies on suitable metals in targeted places [30-31]. The inclusion of a cavity near the tunneling junction increases dissolution capacity and enhances ion-conducting abilities, causing the device to have greater sensitivity to charged and uncharged biomolecules. Integrated into the Silvaco ATLAS device simulator, the biosensor successfully identified biomolecules including uricase, glucose oxidase, APTES, bacteriophage T7, keratin, and gelatine. Specifically, the theoretical and simulation studies stress the possibilities to use TFETs such as CS-CPTFET and CD-CPTFET biosensors to develop bioelectronics for biomolecule detection.

Published by :
http://www.ijert.org

International Journal of Engineering Research & Technology (IJERT)
ISSN: 2278-0181
Vol. 13 Issue 08, August-2024

II. PROPOSED DEVIXE ARCHITECTURE

In the field of biosensors using Charge Plasma TFET, we've developed two unique devices: The proposed device is named as Cavity on Source Charge Plasma TFET (CS-CPTFET) and the Cavity on Drain Charge Plasma TFET (CD-CPTFET) It includes source (LS) and drain (LD) extensions of length 40 nm. For channel length (LC), it effectively chosen to be 20 nm. There is a small empty space which is Vacancy that is situated between the source and one of the layers of SiO2 designed to host biomolecules. This cavity, which is designed to contain biomolecules, has a length of 8 nm and a thickness of 5 nm although it is not symmetrical as it seems from Fig. Our source metal is Platinum with a work function of 5.93 eV while that of the drain metal is Hafnium with a work function of 3.93 eV. The gate metal work function is determined to be 4.5 eV. To enhance the bonding of biomolecules within the nanogaps, semiconducting material SiO2 is incorporated whose thickness is maintained to be 0.5 nm. This sacrificial layer not only helps to improve the biomolecule sticking to the channel but also effectively reduces the leakage current between the gate and the channel further improving the device performance.

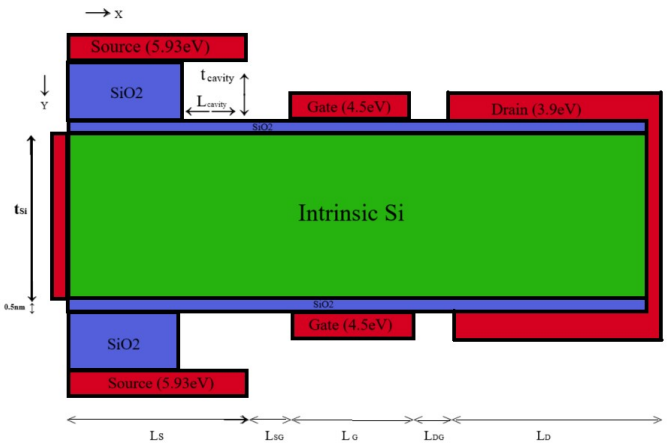

Fig1. Transversal view of CS-CPTFET Biosensor

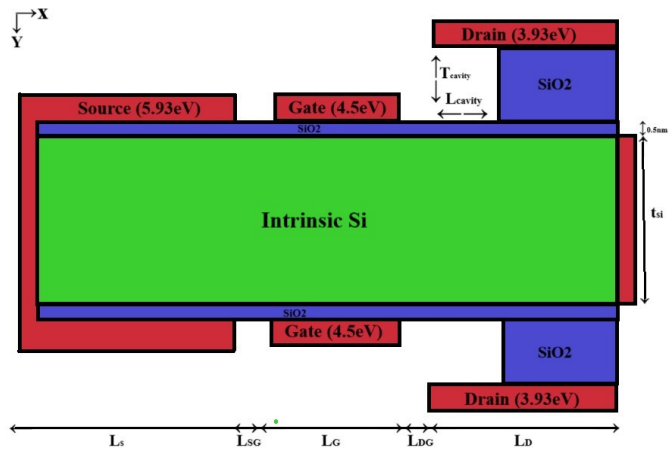

Fig2. Transversal view of CD-CPTFET Biosensor

TABLE I Various Biomolecules with Dielectric Constant

Biomolecules	Dielectric Constant
Uricase	1.54
Biotin	2.63
3-aminopropyltrieth Oxysilane (APTES)	3.57
Bacteriophage T7	6.3
Keratin	6
Gelatin	12

Fig 1(a). Silicon, Fig 1(b). Add SiO2 on both sides.

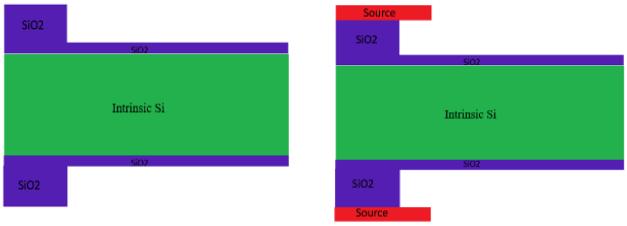

Fig 1(c). Thicker SiO2 on the Source side for introducing cavity.

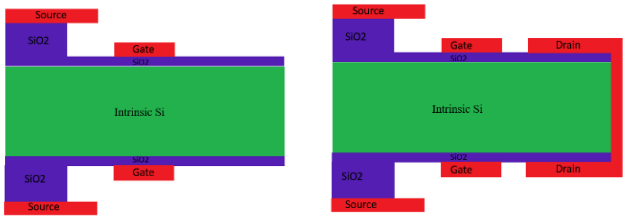

Fig 1(d). Source, Gate and Drain terminals using various.

When developing the CS-CPTFET-based label-free biosensor, we remove a portion of the source material and carve it out during the technology fabrication stage as the cavities it produces are beneficial. A very thin 0.5 nm adhesive layer of SiO2 is formed by dry oxidation that eliminates the formation of silicide also. All the source, gate and drain electrodes are carefully designed using a low-pressure chemical vapor deposition (LPCVD). It is imperative to note that the internal doping concentration has been taken as 1018 cm−3 of the whole extent of the device. The nanogaps, which are crucial components of biosensing structures, are equally and strategically etched on the source dielectric layer as can be seen from the design.

During the fabrication process, it has intentionally not included doping at the drain and source regions of the device using Hafnium (3. 9 eV) drain metal and Platinum (5. 93 eV) source metal. These metals are selected based on the charge plasma

International Journal of Engineering Research & Technology (IJERT)
ISSN: 2278-0181
Vol. 13 Issue 08, August-2024

where the metal for the drain can be chosen only if $\phi D < \chi Si + Eg2$, and for the source metal, $\phi S > \chi Si + Eg2$ where χSi is the electron affinity of the silicon is 4.17 eV, and Eg is the band gap of silicon 1.1eV. In this design, the silicon body has tsi (thickness) of 10 nm which follows Debye's length to provide the desired smooth functionality without entering the quantum domain. The proposed biosensor that uses the CD-CPTFET is shown to have the same level of efficiency as Device 1. This also comprises of source (Ls), drain (LD) of dimensions 40 nm each, and a uniform channel length (LC) of 20 nm. As shown in Fig. 2, a cavity is also incorporated at the CD-CPTFET biosensor structure, to be located between the drain and the SiO2 layer which will be etched away. This cavity meant for accommodating biomolecules also retains the length (Lcavity) of 8 nm as well as the thickness of (Tcavity) of 5 nm.

The source metal, Platinum with work function of 5.93 eV, and the drain metal, Hafnium, with work function of 3.93 eV has been selected very carefully. The gate metal work function is also set at 4.5eV for all the designs as a benchmark value. The adhesion of biomolecules within the nanogaps is ideally ensured by SiO2 that is used as a dielectric material with thickness of 0.5 nm. In the process of fabricating the CD-CPTFET-based label-free biosensor, there are special shaped cavities in the drain dielectric layer which are etched by dry etching process. In the same vein, a very thin 0.5nm SiO2 layer of adhesive layer is created through dry oxidation which helps in avoiding formation of silicide. In both these devices, these highly detailed structural descriptions are directed towards accurate biosensing, stability of biomolecular attachment, consistency of device dimensions, counteracting gate leakage current for optimal functioning and incorporating different biomolecules for checking sensitiveness.

Fig 2(a). Silicon, Fig 2(b). Adding SiO2 on both sides.

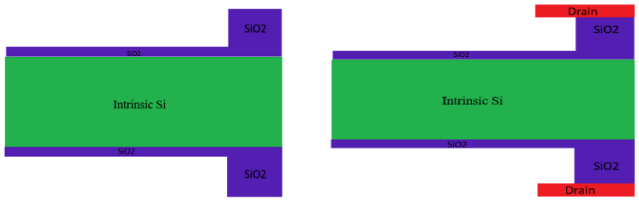

Fig 2(c). Thicker SiO2 on the Drain side.

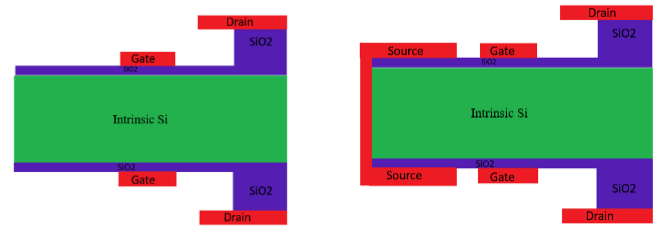

Fig 2(d). Source, Gate and Drain terminals using various metal work functions.

TABLE II

Component	Symbol	Value	Unit
Source length	L_S	40	nm
Source-gate length	L_{SG}	2	nm
Gate length	L_G	13	nm
Drain-gate length	L_{GD}	5	nm
Drain length	L_D	40	nm
Cavity length	L_C	8	nm
Cavity thickness	t_C	5.5	nm
Silicon thickness	t_{SI}	10	nm
SiO2	L_{SI}	10	nm

III. DEVICE CALIBERATION AND MODELLING

In our work, the Silvaco ATLAS 2D device simulator is employed for detailed simulation of CS-CPTFET (Cavity on Source Charge Plasma Tunnel Field-Effect) and CD-CPTFET (Cavity on Drain Charge Plasma Tunnel Field-Effect). For the simulation of our device, we employed the Silvaco ATLAS 2D device simulator which has been established for its credibility and general use in numerous semiconductor investigations. For our simulations, we were very precise in calculating tunnelling rates, which are essential if one wants to understand how a semiconductor operates. We employ an accurate approach known as nonlocal band-to-band tunnelling (BTBT) model. This model is famous for explaining the process of the transportation of electric charges through semiconductor materials with the help of tunnelling. To effectively replicate the quantum tunnelling at the source-channel and drain-channel interfaces, sometimes termed as the tunnelling junctions, of both CS-CPTFET and CD-CPTFET, two quantum tunnelling areas are incorporated specifically for each device. These regions are major in carrier tunnelling which is one of the basic mechanisms in semiconductor devices. In illustrating our argument, we wish to focus on the fact that a more elaborate grid should be used in the places where quantum tunneling occurs. This is important to get proper sensitivity values and to guarantee to ourselves and to the reader that our simulations are as reliable as possible. In this simulation, we show how concentration and electric field can influence the transport of the charge carriers in semiconductors. Semiconductor materials come with a matter of charge carriers moving around inside it, and we have Lombardi mobility model, which explains this phenomenon.

To model recombination of these represented minority carriers, both Shockley–Read–Hall and Auger recombination models are included into the simulation for the CS-CPTFET and CD-CPTFET. The recombination process which happens when two of the charges get together and let off energy has a considerable impact on semiconductor devices. This calls for accurate modelling of these processes if one is to have a realistic and reliable outcome of the simulation. It should also be noted that in our proposed simulation framework we also take into consideration the effect known as bandgap narrowing and use

International Journal of Engineering Research & Technology (IJERT)
ISSN: 2278-0181
Vol. 13 Issue 08, August-2024

the Fermi–Dirac statistics for both the laser and the modulator. These incorporate a significant part to control charge carrier behavior within the semiconductor material making them part of our simulation for accuracy.

In all these devices, we employ a numerical method known as the Wentzel-Kramers-Brillouin (WKB) method to compute tunneling probability. This method enables us to compute the probability of charge carriers tunnel through the potential energy barriers which are characteristic of both devices. Hence, in the following sections, validation is done to check the authenticity and accuracy of our both CS-CPTFET and CD-CPTFET simulations. Notably, we compare our simulated transfer characteristics at VDS = 1V with those in previous works of Kumar and Janardhanan who have also used conventional doping-less TFET models [32]. Thus, the rather close match of our simulated outcomes to the conventional benchmarks that we deployed constitutes rather compelling confirmation of the reliability and accuracy of our simulator for these two devices.

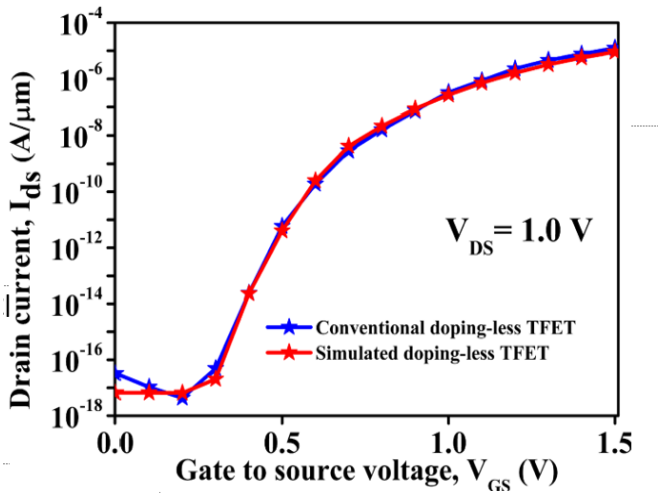

Fig3. Evaluation with conventional doping-less TFET [32]

IV. RESULTS AND DISCUSSION

The findings from CS-CPTFET and CD-CPTFET show interesting responses. They relate to both charged & neutral biomolecules. In all these cases, the Dielectric constant value stays at 1. This means k = 1, which helps get the widest tunnelling barrier. This is important because, when we look at this kind of application, we know that other charged & neutral molecules can fit inside the cavity. This boosts the coupling capacitance under the source electrode for CS-CPTFET and under the drain electrode for CD-CPTFET. We can really see how well the biosensor works by swapping out the air gap with biomolecules in the cavity. That happens under the source electrode for CS-CPTFET and under the drain electrode for CD-CPTFET. The results talk about carrier density, surface potential, band energies, transfer characteristics, ION/IOFF ratios, plus subthreshold swing (SS). In this paper, we explore using the charge plasma concept. It helps us look at carrier concentration in various regions like the source, channel, and drain when it's OFF (VGS = 0 V, VDS = +1.0 V) and ON (VGS = +1.5 V, VDS = +1.0 V). We assume that if the channel length is shorter than the carrier's mean free path, then we can get a hole carrier concentration of about 10^{20} cm^{-3} in the source area & about 10^{20} cm^{-3} for electron carrier concentration in the drain area—both happening under OFF & ON states.

It's clear that when the device is in the ON state, electrons build up in the channel. This happens because of the gate biasing, leading to a quicker tunnelling rate. Now, the Figure 4(a) shows how hole concentration changes in the source area with different dielectric constants of neutral biomolecules. What's interesting is that the capacitive coupling between the source region and its electrode (Platinum) changes along with the dielectric constant of these biomolecules. Why does this matter? Well, the dielectric constant tells us how much electric fields can be stored in a material. So, if a biomolecule has a high dielectric constant, it means it can hold more electric field. Therefore, the capacitive coupling goes up.

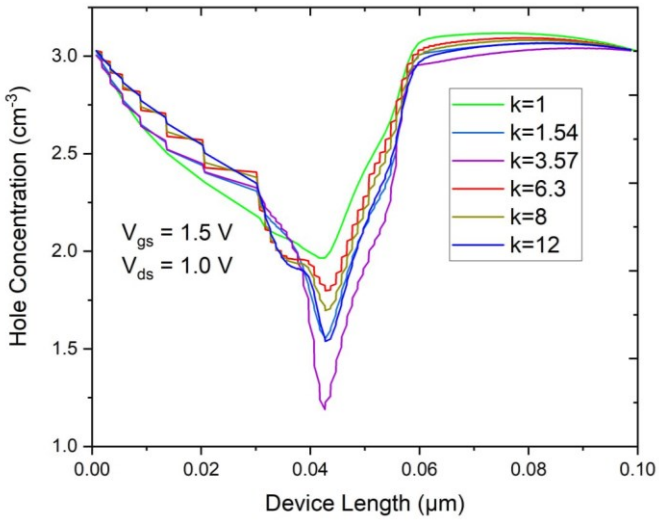

Fig 4(a). Hole concentration variation in source region due to neutral biomolecules

These stronger capacitive couplings in turn translate to higher hole concentration underneath the cavity and therefore cause an abrupt junction (abrupt doping profile) between the channel and the source. This is because holes are attracted to an electric field produced by the biomolecules and the more the electric field the more the holes. In Fig 4(b) the oscillation of hole concentration in the source region due to presence of charged biomolecules. The origin of negative charges of biomolecules attracts more holes to the source region when negatively biomolecules are being trapped into the cavities the steepest gradient at the source-channel (tunnelling junction). This is since the biomolecules contain negative charges and thus produce an electric field that will attract the holes.

International Journal of Engineering Research & Technology (IJERT)
ISSN: 2278-0181
Vol. 13 Issue 08, August-2024

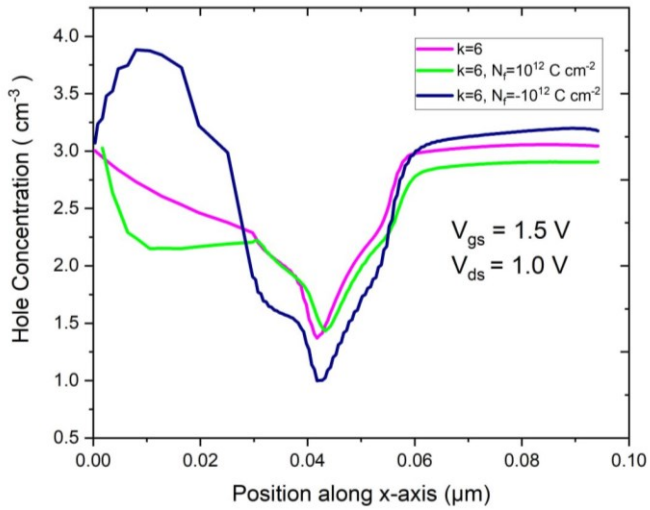

Fig 4(b). Hole concentration variation in source region due to charged biomolecules

On the other hand, when positively charged biomolecules are trapped into the cavities they are repelled by the holes and therefore causes a decrease in the hole concentration at the source region. This is because the biomolecules positive charges impede the development of an electric field that tends to repel the holes. The distribution of the band energy for the device along its length when it is in the OFF state and the ON state are also clearly shown in our analysis. The Energy band diagram is given in Figure 5(a) especially for the CS-CPTFET. Notably missing is any indication of band alignment of the valence band of the source with the conduction band of the channel for any of the biological cavity configurations, including the biomolecules case where the cavity is filled with biomolecules.

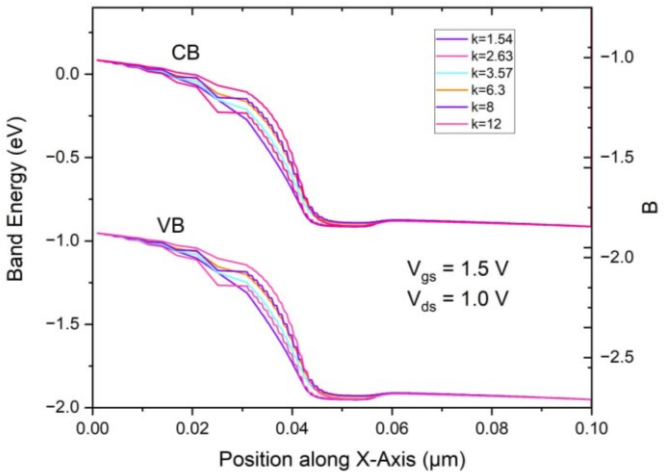

Fig 5(a). Band energy variation of CS-CPTFET due to neutral biomolecules

Consequently, we get fewer holes in the source region and this widening makes it easier for a particle to cross over to the sink region. When there are positively charged biomolecules inside the empty space, they attract electrons towards them and thus the voltage regulation between the source electrode and the source region declines. As a result, it leads to a decrease in sudden doping which is essential for the growth of the company. However, it is crucial to point out that abrupt doping presupposes enhancement of the negatively charged density of biomolecules in the cavity.

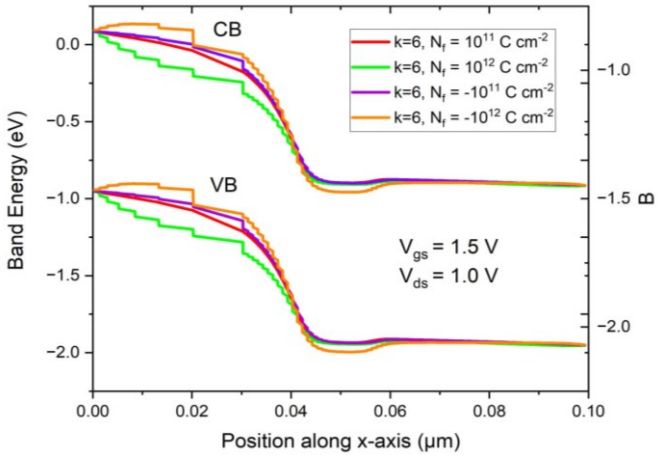

Fig 5(b). c Band energy variation of CS-CPTFET due to charged biomolecules.

Therefore, the lowering of tunnelling barrier is much more reflected in the CS-CPTFET when negatively charged biomolecules are involved. The increase of the dielectric constant values within the biomolecule filled cavities corresponds to an increase in the hole density in the source region The higher number of holes (effectively, the lack of electrons) under the empty space enables the Valence Band and the Conduction Band in the material to align or 'meet' within a much easier way.

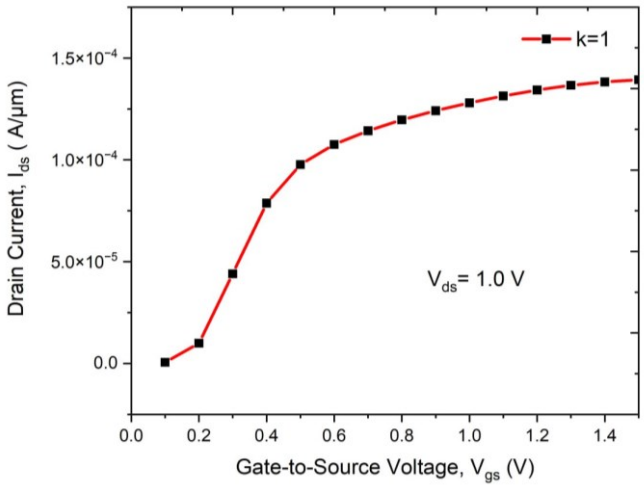

Fig6(a). Transfer characteristics of CS-CPTFET due to Neutral biomolecules

This forms the basis of the increase in the ON current with a resultant enhancement of electron tunnelling due to the decrease of the tunnelling barrier. Fig 6(a) shows the drain current recorded for the CS-CPTFET with air (k=1) biomolecules for the sake of comparison. The new model effectively avoids the phenomenon of ambipolar conduction, and its maximum current is 1. 25 x 10^{-4} A/μm. On the other hand, if there are negatively charged biomolecules in the empty spaces they pull or attract a larger number of holes towards them. This effect increases the source impurity

International Journal of Engineering Research & Technology (IJERT)
ISSN: 2278-0181
Vol. 13 Issue 08, August-2024

concentration to promote the decrease of tunnelling barrier and increase the rate of tunnelling. Thus, as there is a high amount of negative charge, the current going "ON" also increases as observed at figure 6(b).

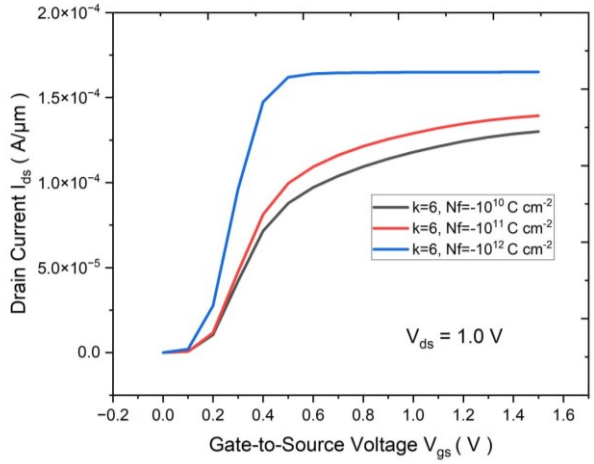

Fig 6(b). Transfer characteristics of CS-CPTFET due to Negative charged biomolecules.

A doping profile that corresponds to an increase of the dielectric values of the immobilized biomolecules within the cavities lead to an improvement of the electric field at the tunnelling junction

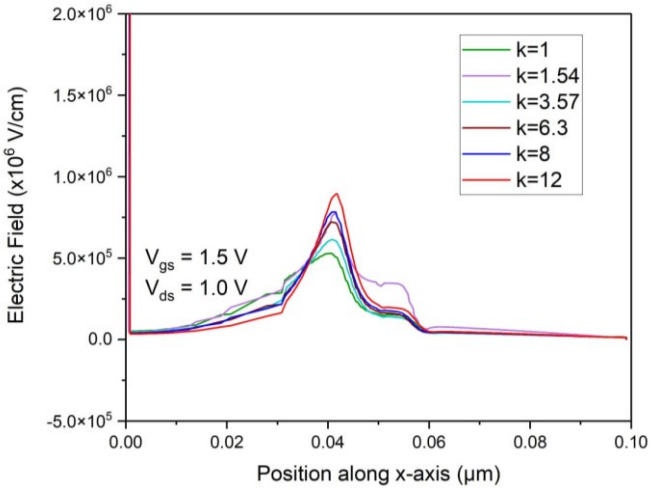

Fig7(a). Electric field of CS-CPTFET along the device length for neutral biomolecules

Figures shown in 7(a) also shows that with neutral biomolecules in CS-CPTFET, the possibility of an electric field reaches as high as 8. The energy at broad tunnelling junction of the thin layer is 8.95 × 10^5 V/cm when k = 12. Figure 7(b) shows the electric field dependence on positive charge density variation from Nf =10^{10} C cm^{-2} to 10^{12} C cm^{-2}. In this illustration, it is apparent that and as the density of positive increase the electric field decreases since the barrier that particles need to tunnel through increases.

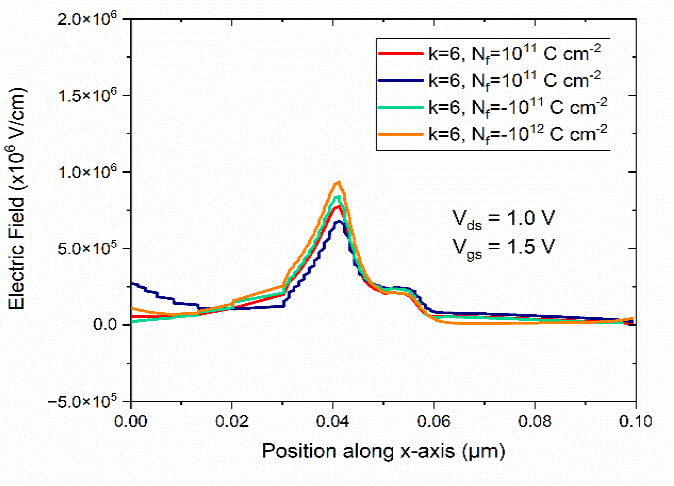

Fig 7(b). Electric field of CS-CPTFET along the device length for charged biomolecules.

On the other hand, whenever there are many negative charges around then one can observe that the electric field is stronger. The variation of electron concentration in the drain region with dielectric constant values of neutral biomolecules has been depicted in fig 8(a). Hence the coupling capacitance between the drain and its electrode (Hafnium) rises with the rising dielectric constant of biomolecules. This is so because the dielectric constant of a material defines the capability of the material for storge of electric field and an increased dielectric constant indicates that the biomolecules can store more of electric field leading to increased coupling capacitance. This increase in coupling capacitance causes an increase electron density underneath the cavity and an abrupt delta doping between the drain and the channel regions. This is the case because electrons are attracted to the biomolecules electric field and the stronger the electric field the more electrons are attracted. As discussed above, the charged biomolecules affect the electron concentration in the drain region, which is depicted in the Fig 8(b).

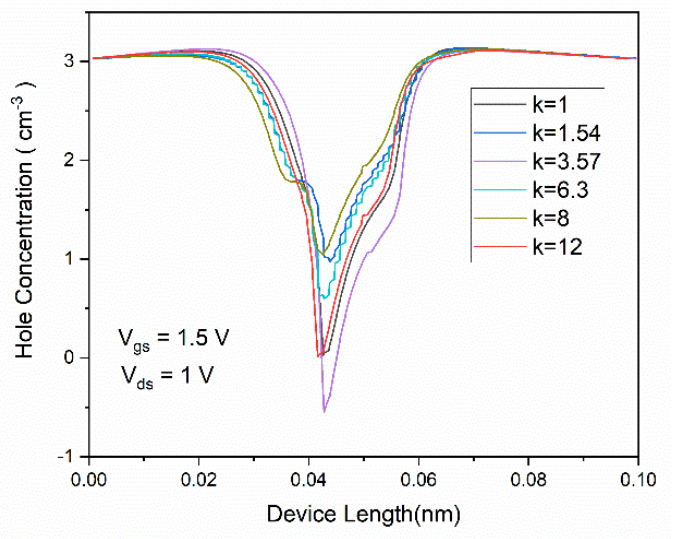

Fig8(a). Hole concentration variation in drain region due to neutral biomolecules.

Published by :
http://www.ijert.org

International Journal of Engineering Research & Technology (IJERT)
ISSN: 2278-0181
Vol. 13 Issue 08, August-2024

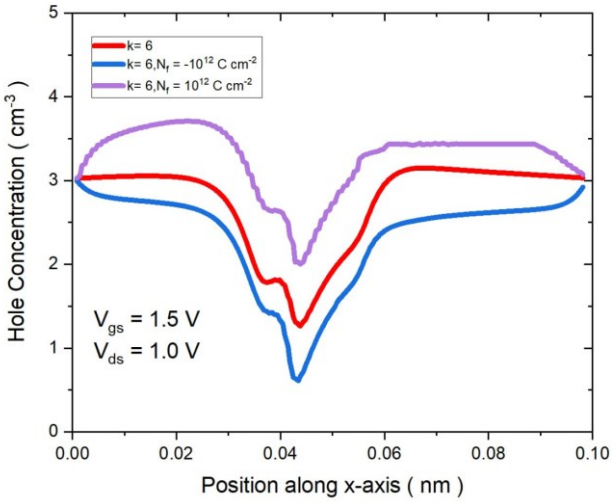

Fig8(b). Hole concentration variation in drain region due to charged biomolecules

When positive charged biomolecules are trapped into the cavities they collect more electrons into the drain region, thereby creating a steepness at the tunnelling junction (drain-channel). This remains so since the biomolecules bearded positive charges therefore meaning that an electric field forms to attract the electrons. On the other hand, when the negative charged biomolecules are entrapped into the cavities, it repels the electrons which in turn reduces the electron density in the drain region. This is due to the biomolecule's negative charges, which causes the biomolecules to build an electric field that repels electrons. It is now significant to see how the existence of biomolecules altered the band energy away from the CD-CPTFET device both in the OFF and ON states. As illustrated in the mainly Figure 9(a) presenting the Energy band diagram for the purpose of representing the said effects, a diagram that is exclusively designed for the CD-CPTFET has been provided below. On a closer examination, there is no proper alignment of energy levels between the source's valence band and the channel's conduction band, not even when the empty space is packed densely with biomolecules.

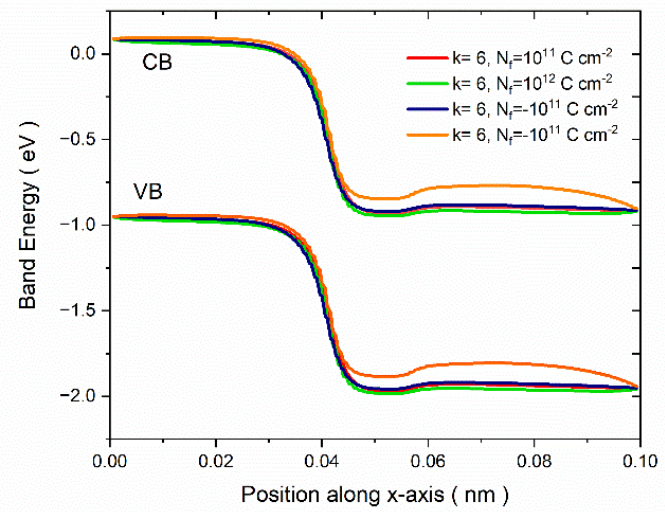

Fig.9(a) Band energy variation of CD-CPTFET due to neutral biomolecules.

Whenever there is an increase in the dielectric constant then the width of the barrier through which particles must tunnel through experiences a great reduction. This is rather an interesting happening because there are more electrons focused within the source region that enhances the rate of tunneling current. The next one is Fig 9(b), Let me explain the details of this. From this figure, it is evident that another pattern is the fact that as the width of the barrier that the particles have to tunnel through increases. This phenomenon occurs due to the availability of negative biomolecules within the cavity of the said carbon structure.

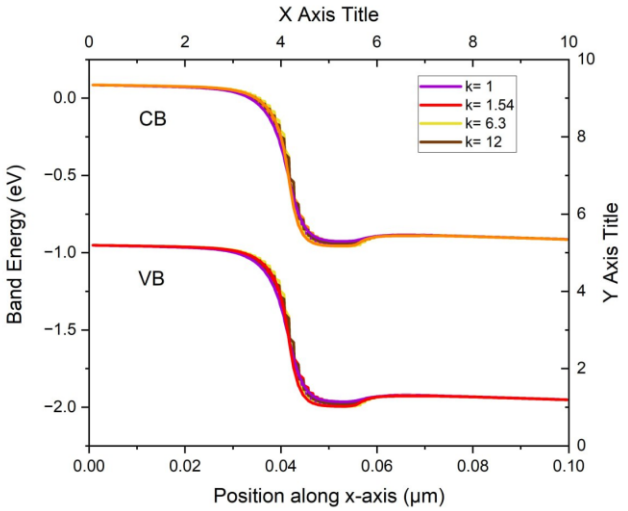

Fig.9(b) Band energy variation of CD-CPTFET due to charged biomolecules

What is even more favorable for the device operational capabilities is that such widening also shifts the hole concentration in the drain area even lower. The negatively charged biomolecules deployed at the cavity create an electrostatic attraction force on the electrons reducing the control voltage between the drain electrode and the drain region. This in the process helps in decreasing situations where there is abrupt doping. However, it is important to note that only with the increased density of positive ions of biomolecules is it possible to achieve abrupt doping in CD-CPTFET. The obtained dielectric constant values closer to the biomolecule-filled cavities enables a higher electron density within the drain region. This results into an effective matching of the Valence Band and the Conduction Band in the material due to increase in the number of electrons under the empty space. This alignment results to a decrease of the tunnelling barrier and increase in hole tunnelling, thus the ability to increase ON current. As a reference, the normalized plots of the drain current of the CD-CPTFET with air (k=1) biomolecules are shown in figure 10(a).

Published by :
http://www.ijert.org

International Journal of Engineering Research & Technology (IJERT)
ISSN: 2278-0181
Vol. 13 Issue 08, August-2024

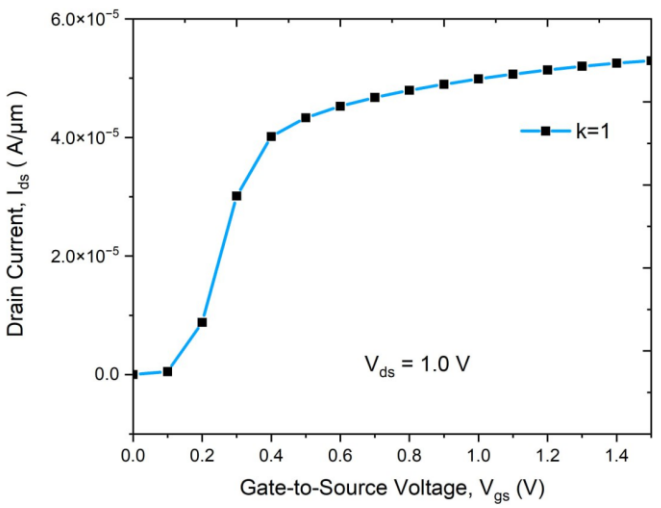

Fig 10(a). Transfer characteristics of CD-CPTFET due to Neutral Biomolecules.

Notably, inherent ambipolar conduction is significantly minimized in the proposed model while it reaches a maximum current density of 5.23 x 10^{-5} A/μm. On the other hand, when such empty spaces have positively charged biomolecules inside, such molecules pull or attract a larger volume of electrons toward them. This effect improves the concentration of the drain impurity that enables a decrease in the tunnelling barrier and hence the tunnelling rate. Consequently, the current which flows through the device when the switch is in the "ON" position rises right alongside the increase in the quantity of negative charges, which is depicted in Fig 10(b). It is big that one creates a particular doping pattern to correspond with the higher dielectric values of the biomolecules within the empty spaces. It increases linearly the strength of the electric field at the tunnelling junction by a factor that is immensely large compared to the additional energy provided by the magnetic field also enhances the strength of the electric field at the tunnelling junction.

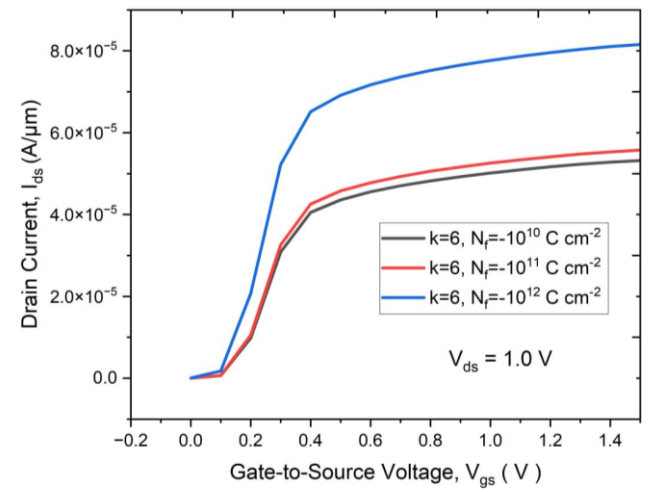

Fig 10(b). Transfer characteristics of CD-CPTFET due to Negative charged biomolecules.

There the electric field is largely enhanced and the strength at the tunneling junction is increased. From the observation made in Figure 11(a), it is evident that the applied electric field in the CD-CPTFET employing neutral biomolecules shows the possibility of achieving a highly intense electrical field that can go up to 2.25 × 10^6 V/cm at the tunnelling junction when dielectric constant (k) becomes equal to 12. Fig 11(b) explains how the variation of positive charge density of range Nf = 10^{10} C cm^{-2} to 10^{12} C cm^{-2} affects the electric field. While comparing the effects of an increase in positive charge density in this graphical representation one becomes very much aware that the electric field decreases since the width of the tunnelling barrier has increased. On the other hand, there is an augmentation of the electric field as the negative charge density increases. Since sensitivity serves as a basic assessment criterion for a biosensor, it is intuitively perceived as a critical component in the biosensor construction as well as assessment.

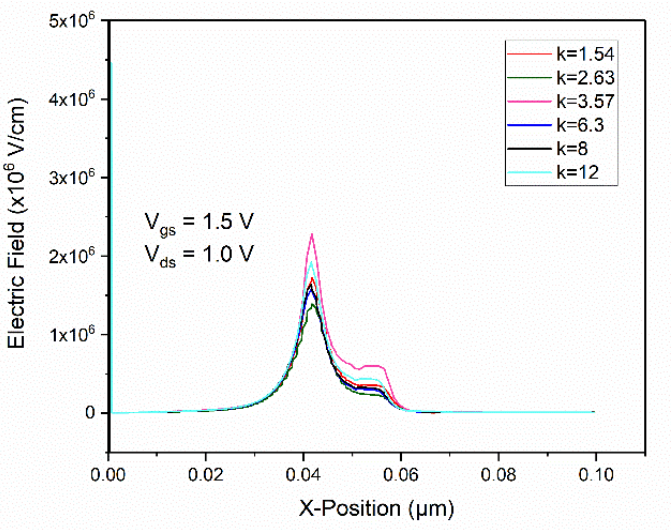

Fig 11(a). Electric field of CD-CPTFET along the device length for neutral biomolecules.

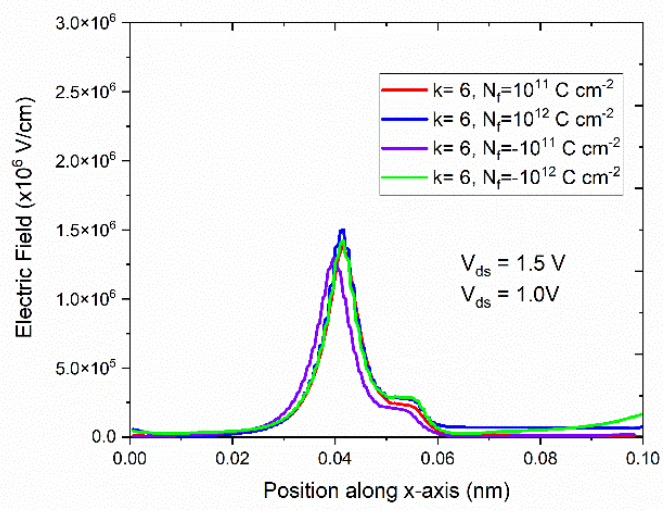

Fig 11(b). Electric field of CD-CPTFET along the device length charged biomolecules.

International Journal of Engineering Research & Technology (IJERT)
ISSN: 2278-0181
Vol. 13 Issue 08, August-2024

Thus, a high sensitivity value means that the biosensor is very effective in its capacity to accurately identify the specific biomolecule it is intended to detect. As for the biosensing performance of the CD-CPTFET biosensor, sensitivity is defined by the drain current, and the variation of the current is only attributable to the charged and the neutral biomolecules. Performance of this important parameter involves the following formula as described in [30].

$$S_{I_{ds}} = \left(\frac{I_{ds}^{bio} - I_{ds}^{air}}{I_{ds}^{air}} \right)$$

The Equation serves to distinguish between two scenarios: one with empty cavities, resulting in a drain current labelled as I_{ds}(air), and the other with filled cavities, yielding the drain current denoted as I_{ds}(bio). Consequently, the CD-CPTFET biosensor is employed to calculate sensitivity values for various biomolecules.

Table III

Employed Biomolecules	Dielectric Constant(k)	Sensitivity (V_{GS}=1.5V and V_{DS}=1.0V)
Neutral Biomolecules	1.54	9.5×10^{-3}
	3.57	1.33×10^{-3}
	6.3	1.13×10^{-2}
	12	1.14×10^{2}
Charged Biomolecules	k=6, N_f=-10^{10}C/Cm^2	5.6×10^{-3}
	k=6, N_f=-10^{11}C/cm^2	6.5×10^{-2}
	k=6, Nf=-10^{12}C/cm^2	5.5×10^{9}

It's worth noting that biomolecules characterized by higher dielectric constants (k > 1) exhibit a concurrent rise in drain current (I_{ds}). This increase in drain current corresponds directly to heightened levels of sensitivity. Table 3] shows the sensitivity values of neutral and charged biomolecules of the CD-CPTFET.

V . CONCLUSION

We have designed innovative sensors capable of accurately detecting various substances without the need for specialized labels. These sensors, known as CS-CPTFET and CD-CPTFET, were enhanced with unique features under the electrodes, resulting in exceptional performance. Our experiments demonstrated the effectiveness of these sensors in discerning different substances with precision. Both CS-CPTFET and CD-CPTFET sensors exhibited impressive detection capabilities. CS-CPTFET achieved a current detection of 1.5 x 10-4 A per small unit, while CD-CPTFET detected substances with a current of 5.23 x 10-5 A per small unit. We came to a conclusion that there is not much variation in the sensitivity for the CD-CPTFET compared to CS-CPTFET. These sensors are versatile and robust, making them suitable for various applications in fields such as medical testing, environmental monitoring, and the food industry. Moreover, our work offers valuable clues for creating even better sensors in the future. These improvements will make substance detection more precise and sensitive without needing labels. This work signifies not only a significant contribution to the field of biosensors but also a pathway to future innovations in substance detection.

REFERENCES

[1] A. Manickam, A. Chevalier, M. McDermott, A. D. Ellington and A. Hassibi, "A CMOS electrochemical impedance spectroscopy biosensor array for label-free biomolecular detection," 2010 IEEE International Solid-State Circuits Conference - (ISSCC), San Francisco, CA, USA, 2010, pp. 130-131, doi: 10.1109/ISSCC.2010.5434019J.

[2] R. Kumari, P. N. Patel and R. Yadav, "An ENG-Inspired Microwave Sensor and Functional Technique for Label-Free Detection of Aspergillus Niger," in IEEE Sensors Journal, vol. 18, no. 10, pp. 3932-3939, 15 May15, 2018, doi: 10.1109/JSEN.2018.2822306.

[3] K. N. Priyadarshani and S. Singh, "Ultra Sensitive Label-Free Detection of Biomolecules Using Vertically Extended Drain Double Gate $Si_{0.5}Ge_{0.5}$ Source Tunnel FET," in IEEE Transactions on NanoBioscience, vol. 20, no. 4, pp. 480-487, Oct. 2021, doi: 10.1109/TNB.2021.3106333.

[4] Manaswi D., Karumuri S.R., Wadhwa G., "Design and Parametric Analysis of Charge Plasma Junctionless TFET for Biosensor Applications," 2023 IEEE Open Journal of Nanotechnology, vol. 4, pp. 71-76, doi: 10.1109/OJNANO.2022.3224462.

[5] P. Bergveld, "Development of an ion-sensitive solid-state device for neurophysiological measurements," IEEE Trans. Biomed. Eng., vol. BME-17, no. 1, pp. 70–71, Jan. 1970.

[6] S. Dhar, B. Maji, S. Das, M. Das and S. J. Mukhopadhyay, "Relative Study on Performance analysis of DMFET and DMTFET based Transducers," 2023 International Conference on Computer, Electrical & Communication Engineering (ICCECE), Kolkata, India, 2023, pp. 1-4, doi: 10.1109/ICCECE51049.2023.10085414.

[7] Aditya M., Rao K.S., "Impact of High-K Gate Dielectric Materials on Uniformly Doped Dual Gate FinFET for Analog and Digital Applications," 2022 Silicon, vol. 14, no. 16, pp. 10623-10635, doi: 10.1007/s12633-022-01775-8.

[8] Kumar P.K., Balaji B., Rao K.S, "Design and analysis of asymmetrical low-k source side spacer halo doped nanowire metal oxide semiconductor field effect transistor," 2023 International Journal of Electrical and Computer Engineering., vol. 13, no. 3, pp. 3519-3529, doi: 10.11591/ijece.v13i3.pp3519-3529.

[9] Kumar P.K., Balaji B., Rao K.S., "Halo-Doped Hetero Dielectric Nanowire MOSFET Scaled to the Sub-10Â nm Node," 2023 Transactions on Electrical and Electronic Materials., vol. 24, no. 4, pp. 303-313, doi: 10.1007/s42341-023-00448-6.

[10] K. Hui, C. Hu, P. George and P. K. Ko, "Impact ionization in GaAs MESFETs," in IEEE Electron Device Letters, vol. 11, no. 3, pp. 113-115, March 1990, doi: 10.1109/55.46951.

[11] [D. B. Abdi and M. Jagadesh Kumar, "Controlling Ambipolar Current in Tunneling FETs Using Overlapping Gate-on-Drain," in IEEE Journal of the Electron Devices Society, vol. 2, no. 6, pp. 187-190, Nov. 2014, doi: 10.1109/JEDS.2014.2327626.

[12] [12] A. Shaker, M. El Sabbagh and M. M. El-Banna, "Influence of Drain Doping Engineering on the Ambipolar Conduction and High-Frequency Performance of TFETs," in IEEE Transactions on Electron Devices, vol. 64, no. 9, pp. 3541-3547, Sept. 2017, doi: 10.1109/TED.2017.2724560.

[13] [Y. -F. Chen, L. -W. Hsu, C. -W. Hu, G. -T. Lai and Y. -H. Wu, "Enhanced Tunneling Electro-Resistance Ratio for Ferroelectric Tunnel Junctions by Engineering Metal Work Function," in IEEE Electron Device Letters, vol. 43, no. 2, pp. 208-211, Feb. 2022, doi: 10.1109/LED.2021.3133577.

[14] Yee-Chia Yeo, P. Ranade, Tsu-Jae King and Chenming Hu, "Effects of high-/spl kappa/ gate dielectric materials on metal and silicon gate workfunctions," in IEEE Electron Device Letters, vol. 23, no. 6, pp. 342-344, June 2002, doi: 10.1109/LED.2002.1004229.

International Journal of Engineering Research & Technology (IJERT)
ISSN: 2278-0181
Vol. 13 Issue 08, August-2024

[15] ATLAS Device Simulation Software, Silvaco, Santa Clara, CA, USA, 2016.
[16] M. Patil, A. Gedam and G. P. Mishra, "Performance Assessment of a Cavity on Source ChargePlasmaTFET-Based Biosensor," in IEEE Sensors Journal, vol. 21, no. 3, pp. 2526-2532, 1 Feb.1, 2021, doi: 10.1109/JSEN.2020.3027031.
[17] J. Ahn, W. Ting and D. . -L. Kwong, "High-quality MOSFETs with ultrathin LPCVD gate SiO/sub 2/," in IEEE Electron Device Letters, vol. 13, no. 4, pp. 186-188, April 1992, doi: 10.1109/55.145015.
[18] B. Rajasekharan, R. J. E. Hueting, C. Salm, T. van Hemert, R. A. M. Wolters and J. Schmitz, "Fabrication and Characterization of the Charge-Plasma Diode," in IEEE Electron Device Letters, vol. 31, no. 6, pp. 528-530, June 2010, doi: 10.1109/LED.2010.2045731.
[19] R. Narang, M. Saxena and M. Gupta, "Comparative Analysis of Dielectric-Modulated FET and TFET-Based Biosensor," in IEEE Transactions on Nanotechnology, vol. 14, no. 3, pp. 427-435, May 2015, doi: 10.1109/TNANO.2015.2396899.
[20] S. Anand, A. Singh, S. I. Amin and A. S. Thool, "Design and Performance Analysis of Dielectrically Modulated Doping-Less Tunnel FET-Based Label Free Biosensor," in IEEE Sensors Journal, vol. 19, no. 12, pp. 4369-4374, 15 June15, 2019, doi: 10.1109/JSEN.2019.2900092.
[21] A. Cuervo, P. D. Dans, J. L. Carrascosa, M. Orozco, G. Gomila, and L. Fumagalli, “Direct measurement of the dielectric polarization properties of DNA,” Proc. Nat. Acad. Sci. USA, vol. 111, no. 35, pp. E3624–E3630, Aug. 2014.
[22] S. Kim, D. Baek, J.-Y. Kim, S.-J. Choi, M.-L. Seol, and Y.-K. Choi, “A transistor-based biosensor for the extraction of physical properties of from biomolecules,” Appl. Phys. Lett., vol. 101, no. 7, Aug. 2012, Art. no. 073703.
[23] A. Paliwal, M. Tomar, and V. Gupta, “Complex dielectric constant of various biomolecules as a function of wavelength using surface plasmon resonance,” J. Appl. Phys., vol. 116, no. 2, Jul. 2014, Art. no. 023109.
[24] R. Goswami and B. Bhowmick, “Comparative analyses of circular gate TFET and heterojunction TFET for dielectric-modulated label-free biosensing,” IEEE Sensors J., vol. 19, no. 21, pp. 9600–9609, Nov. 2019.
[25] N. Colloch et al., “Crystal structure of the protein drug urate oxidaseinhibitor complex at 2.05 Å resolution,” Nature Struct. Mol. Biol., vol. 4, 514no. 11, pp. 947–952, Nov. 1997.
[26] G. Wadhwa and B. Raj, “Label free detection of biomolecules using charge-plasma-based gate underlap dielectric modulated junctionless TFET,” J. Electron. Mater., vol. 47, no. 8, pp. 4683–4693, Aug. 2018.
[27] V. D. Wangkheirakpam, B. Bhowmick, and P. D. Pukhrambam, “N+ pocket doped vertical TFET based dielectric-modulated biosensor considering non-ideal hybridization issue: A simulation study,” IEEE Trans. Nanotechnol., vol. 19, pp. 156–162, 2020.
[28] R. J. E. Hueting, B. Rajasekharan, C. Salm, and J. Schmitz, “The charge plasma P-N diode,” IEEE Electron Device Lett., vol. 29, no. 12, pp. 1367–1369, Dec. 2008.
[29] C. Sahu and J. Singh, "Charge-Plasma Based Process Variation Immune Junctionless Transistor," in IEEE Electron Device Letters, vol. 35, no. 3, pp. 411-413, March 2014, doi: 10.1109/LED.2013.2297451.
[30] A. Anam, S. Anand and S. I. Amin, "Design and Performance Analysis of Tunnel Field Effect Transistor With Buried Strained $Si_{1-x}Ge_x$ Source Structure Based Biosensor for Sensitivity Enhancement," in IEEE Sensors Journal, vol. 20, no. 22, pp. 13178-13185, 15 Nov.15, 2020, doi: 10.1109/JSEN.2020.3004050.
[31] P. K. Dubey and B. K. Kaushik, "A Charge Plasma-Based Monolayer Transition Metal Dichalcogenide Tunnel FET," in IEEE Transactions on Electron Devices, vol. 66, no. 6, pp. 2837-2843, June 2019, doi:10.1109/TED.2019.2909182.
[32] M. J. Kumar and S. Janardhanan, “Doping-less tunnel field effect transistor: Design and investigation,” IEEE Trans. Electron Devices, vol. 60, no. 10, pp. 3285–3290, Oct. 2013.
[33] Sravani S.S., Balaji B., Rao K.S., Babu A.N., Aditya M., Sravani K.G., “A Qualitative Review on Tunnel Field Effect Transistor- Operation, Advances, and Applications,” 2022 Silicon, vol, 14, no.15, pp. 9263-9273, doi:10.1007/s12633-022-01660-4
[34] Balaji B., Rao K.S., Aditya M., Sravani K.G.,“Device Design, Simulation and Qualitative Analysis of GaAsP/ 6H-SiC/ GaN Metal Semiconductor Field Effect Transistor,” 2022 Silicon, vol. 14, no. 14, pp. 8449-8454, doi:10.1007/s12633-022-01665-z.
[35] Aditya M., Rao K.S., Balaji B., Sravani K.G., “Comparison of Drain Current Characteristics of Advanced MOSFET Structures - a Review,” 2022 Silicon, vol. 14, no. 14, pp. 8269-8276, doi:10.1007/s12633-021-01638-8
[36] Aditya M., Rao K.S., Sravani K.G., Guha K., “Simulation and Drain Current Performance analysis of High-K Gate Dielectric FinFET,” 2022 Silicon, vol. 14, no. 8, pp. 4075-4078, doi:10.1007/s12633-021-01176-3